Predicting Molecular Weight and Degree of Branching Distribution of Polyethylene for Mixed Systems with a Constrained Geometry Metallocene Catalyst in Semibatch and Continuous Reactors

Piet D. Iedema* and Huub C. J. Hoefsloot

Department of Chemical Engineering, Universiteit van Amsterdam, Nieuwe Achtergracht 166, 1018 WV Amsterdam, The Netherlands

Received April 1, 2003; Revised Manuscript Received June 23, 2003

ABSTRACT: The problem of finding the bivariate chain length (n)/number of branch points (N) distribution for polyethylene produced by a mixed metallocene catalyst system in continuous (CSTR) and semibatch reactors is addressed in two ways. The first uses distinct classes of chains with a certain number of branches, the second the "pseudodistribution" approach, both generating population balances solved with the Galerkin finite element approach of PREDICI. A nine-classes model yields the exact bivariate distribution up to chains of $n = 10\,000$. Until this limit, classes and pseudodistribution models yield identical results, both being based on identical assumptions. Results also coincide with an analytical solution for a CSTR single catalyst system. In view of their importance for deriving architectures and architectural properties, chain statistics were examined by calculating average segment lengths. In the single catalyst CSTR, these turn out to be independent from the number of branches on a chain, which holds untrue for mixed system CSTRs and *all* semibatch reactors. Concerning the distribution shape of N at fixed n, growing chains at the branching catalyst are always more *narrowly* distributed than a binomial distribution. A new method, the variable power binomial distribution (VPBD), enables a correct description of the branching distribution shape. The model allows performing sensitivity calculations for both reactor systems under varying conditions, including dynamic behavior in a semibatch reactor. The effect of catalyst ratio and hydrogen was explored. The remarkable bimodality in the molecular weight distribution at catalyst ratios around 0.5 already observed before for a semibatch reactor persists in the CSTR.

Introduction

Branched polyethylene has a fascinating rheology, which recently has gained better theoretical understanding by the explicit coupling to its molecular topology.[6,8,26] Gaining a better understanding of the relationship between polymerization kinetics on one hand and rheology on the other is a highly challenging issue. This paper contributes to the issue by focusing on an essential link in this relationship: that between kinetics and the bivariate molecular weight/degree of branching distribution (MWD/DBD) for the case of polyethylene made by a mixed metallocene system.[7] The much older product, low-density polyethylene, has already been the topic of many modeling studies devoted to molecular weight and branching distribution[2] as well as molecular topologies in relation to characterization (radius of gyration) and rheology.[5,9−11] More recently metallocene-catalyzed PE has received attention as regards branching after the discovery of the so-called constrained geometry catalyst (CGC).[12,13] Branches in metallocene systems are formed in a manner quite different from the transfer to polymer in ldPE. β-Hydride elimination and transfer to monomer reactions generate unsaturated chain ends. Because of the open structure of the CGC catalyst these in-situ produced "macromonomers" are incorporated in the growing chain, thus forming long branches. Since its discovery,[12] many experimental and modeling studies have been carried out with the branching catalyst CGC or similar metallocene catalysts.[4,7,14−19] Modeling of ethylene homo and copolymerization has been performed for a CSTR system using the method of moments.[14,15] Full molecular weight and degree of branching distributions (MWD and DBD) have been predicted by both analytical methods and Monte Carlo simulation.[4,16,25] The idea of using a mixed metallocene catalyst system, in which one catalyst would produce chains with terminal double bonds (TDBs) and the other would incorporate them, was raised by Zhu and Li.[20] In their modeling study they predicted the branched structure thus created to possess a mostly "comblike" topology, which yields the product desirable rheological properties. Further studies on mixed metallocene systems focused on prediction of branching using a simple model[23] and rheological characterization of several copolymers.[24] Beigzadeh et al.[7] experimentally tested a mixed system with the branching catalyst CGC−Ti (titanium (N-1,1-dimethylethyl)dimethyl (1-(1,2,3,4,5-η)-2,3,4,5-tetramethyl-2,4-cyclopentadiene-1-yl)silanaminato(2−)-N-dimethyl) and the linear catalyst Et-[Ind]$_2$ZrCl$_2$ (dichloro[*rac*-ethylenebis(indenyl)]zirconium(IV)) in a semibatch reactor. On the basis of MWDs measured by size exclusion chromatography and branching data by NMR spectroscopy, the authors propose that chains with TDBs produced at the linear catalyst are inserted at the branching catalyst. This will be the main system on which we demonstrate the applicability of our new model.

In this paper, we present a new and comprehensive model that is able to predict MWD and DBD for mixed metallocene systems in a semibatch and continuous reactors, accounting for all relevant kinetic mechanisms, including transfer to hydrogen. The modeling approach chosen is a Galerkin FEM method[3] that solves population balances. For a fairly complicated system like the present one, it is not yet possible to solve the full bivariate chain length/degree of branching problem directly. We will employ the "pseudodistribution" approach, developed by us for the case of low-density

10.1021/ma034405q CCC: $25.00
Published on Web 07/29/2003

Table 1. Reaction Mechanisms and Rate Coefficients

reaction	reaction equation	rate coeff
CGC−Ti activation and initiation[a]	$C_{CGC} \rightarrow C^*_{CGC}$	$k_{a,CGC}$
	$C^*_{CGC} + M \rightarrow R^b_{1,0}$	$k_{i,CGC}$
$Et[Ind]_2ZrCl_2$ activation and initiation[a]	$C_{lin} \rightarrow C^*_{lin}$	$k_{a,lin}$
	$C^*_{lin} + M \rightarrow R^l_{1,0}$	$k_{i,lin}$
propagation CGC−Ti	$R^b_{n,i} + M \rightarrow R^b_{n+1,j}$	$k_{p,CGC}$
propagation $Et[Ind]_2ZrCl_2$	$R^l_{n,i} + M \rightarrow R^l_{n+1,j}$	$k_{p,lin}$
β-hydride elimination CGC−Ti	$R^b_{n,i} \rightarrow C^*_{CGC} + P^{b=}_{n,i}$ [b]	$k_{\chi,CGC}$
β-hydride elimination $Et[Ind]_2ZrCl_2$	$R^l_{n,i} \rightarrow C^*_{lin} + P^l_{n,i}$ [b]	$k_{\chi,lin}$
transfer to monomer CGC−Ti	$R^b_{n,i} + M \rightarrow C^*_{CGC} + P^{b=}_{n,i}$ [b]	$k_{m,CGC}$
transfer to monomer $Et[Ind]_2ZrCl_2$	$R^l_{n,i} + M \rightarrow C^*_{lin} + P^{l=}_{n,i}$ [b]	$k_{m,lin}$
transfer to hydrogen CGC−Ti	$R^b_{n,i} + H_2 \rightarrow C^*_{CGC} + P^{b=}_{n,i}$ [b]	$k_{H,CGC}$
transfer to hydrogen $Et[Ind]_2ZrCl_2$	$R^l_{n,i} + H_2 \rightarrow C^*_{lin} + P^l_{n,i}$ [b]	$k_{H,lin}$
terminal double bond propagation CGC−Ti	$R^b_{n,i} + P^=_{m,j} \rightarrow R_{n+m,j+j+1}$ [b]	$k_{p,TDB}$
catal deact (growing chains) $Et[Ind]_2ZrCl_2$	$R^l_{n,i} \rightarrow C^i_{lin} + P^{l=}_{n,i}$ [b]	$k_{d1,lin}$
catal deact (growing chains) CGC−Ti	$R^b_{n,i} \rightarrow C^i_{CGC} + P^{b=}_{n,i}$ [b]	$k_{dl,CGC}$
catal deact (active catalyst) $Et[Ind]_2ZrCl_2$	$C_{lin} \rightarrow C^i_{lin}$	$k_{d2,lin}$
catal deact (active catalyst) CGC−Ti	$C_{CGC} \rightarrow C^i_{CGC}$	$k_{d2,CGC}$

[a] Catalyst activation and initiation are taken as one step. [b] Note that $P^=_{n,i} = P^{b=}_{n,i} + P^{l=}_{n,i}$. In the dead chain *generating* reactions dead chains are distinguished after their origin, $Et[Ind]_2ZrCl_2$ (l) or CGC−Ti (b). In the TDB propagation reactions they are not distinguished, as they are assumed to be equally reactive.

polyethylene[2] (chain length plus branching) and later also successfully applied to poly(vinyl acetate)[1] (chain length plus terminal double bonds). We also compare it to an alternative application of the Galerkin FEM method that explicitly addresses "classes" of chains with a certain number of branches. The kinetic data are based on the experimental data for a semibatch system from Beigzadeh et al.[7] The bivariate chain length/number of branch points problem has been solved before[4] for the case of a CSTR with a single branching catalyst, yielding an analytical expression. Our model includes this system and yields results coinciding with the analytical model. We notice that computing the bivariate MWD/DBD is a preliminary step to finding, for instance, rheological properties, as it forms the direct basis for predicting molecular *architectures*. In a forthcoming study we will address the synthesis of architectures from MWD/DBD in a manner that has proved itself in the case of ldPE, but here we should briefly discuss the relation between architecture and chain statistics. This issue has been implicitly dealt with in a study devoted to the contribution of segments between branch points to rheological behavior of branched molecules.[6] Such segments may be located at the periphery of molecules, eventually as free dangling segments attached to one branch point only, or at the inside. A rheological ranking of such segments is proposed using so-called "seniority" and "priority" values attributed to segments, such as determining relaxation and elastic behavior of the branched molecules, respectively.[22] Now, basic to the aforementioned rheology study of CGC metallocene-catalyzed PE[6] is the self-similarity of all chains produced. This self-similarity is realized if all chains obey the same statistics, which is only true if one catalyst is employed. However, when dealing with a mixed catalyst system, the situation becomes different. Therefore, in our study, chain statistics is a highly relevant issue to be discussed.

Our paper has the following structure. We start with a presentation of the differential equations describing the population balances of all (distributive) species involved. It is shown how either using the classes or the pseudodistribution approach can solve this system. Then the issue of polydispersity of the branching distribution at fixed chain lengths is discussed. The Results section starts with a comparison of the classes and the pseudodistribution model. This is followed by a section about the chain statistics as predicted by the two models. Finally, we present the results of simulations under a varying catalyst ratio, for both a semibatch and a continuous reactor, in absence or presence of hydrogen. Dynamic effects in the semibatch reactor are included here. We show the full bivariate chain length/degree of branching concentration distribution for the case of a mixed metallocene system in a CSTR in the presence of hydrogen and discuss its validity.

Model Description

Population Balances. The reactions involved in the present mixed $Et[Ind]_2ZrCl_2$/CGC−Ti system have been discussed in a few previous kinetic studies.[7,15] The nowadays most generally accepted mechanisms possibly occurring in any mixed metallocene catalyst system with CGC−Ti are listed in Table 1. A more confined set is applicable to $Et[Ind]_2ZrCl_2$/CGC−Ti. Which mechanisms are accounted for is realized by adjusting the kinetic coefficients, eventually putting them equal to zero. However, one should notice that our model is valid for any mixed metallocene catalyst system with CGC−Ti in all reactor types and under all conditions. A full set of population balance equations is given in the Appendix. The two-dimensional formulation and the one-dimensional formulation on the level of chain length concentrations have been presented in earlier modeling studies.[7,14] In the Appendix, it is explained that we employ a simplified molar balance for monomer. This implies that our model is valid for constant monomer concentration, hence for steady-state operation of a CSTR and for the usual constant monomer pressure operating strategy of a semibatch reactor.[7] The "pseudo-distributions" of the first branching moment are derived in a similar manner as shown in our earlier work on ldPE[2] and poly(vinyl acetate).[3] We now discuss in some more detail the reaction equation concerning the incorporation of macromonomers in growing chains at CGC−Ti, leading to branching, with respect to its mathemati-

cal implementation in the Galerkin FEM code PREDICI:

$$R^{b}_{n,i} + P^{=}_{m,j} \xrightarrow{k_{p,TDB}} R^{b}_{n+m,i+j+1}$$

Here, $R^{b}_{n,i}$ denotes growing chains at the branching catalyst (upper index b) with length n and i branch points. Likewise, $P^{=}_{m,j}$ refers to dead chains with a terminal double bond (upper index =) of length m and j branch points. Note that dead chains with a TDB are generated at both linear and branching catalyst. Throughout this work, it is assumed that all of these chains can be incorporated at CGC, regardless of their origin. The problem in the full two dimensions chain length and number of branches per chain is described by the 2-dimensional population balance equations. Note that the += duet means *a contribution to* the overall balance equation of the respective species.

Consumption of growing chains and chains with a terminal double bond:

$$\frac{dR^{b}_{n,i}}{dt} += -k_{p,TDB}R^{b}_{n,i}\sum_{n=1}^{\infty}\sum_{i=0}^{\infty}P^{=}_{n,i} = -k_{p,TDB}R^{b}_{n,i}\mu^{=}_{0} \quad (1)$$

$$\frac{dP^{=}_{n,i}}{dt} += -k_{p,TDB}P^{=}_{n,i}\sum_{n=1}^{\infty}\sum_{i=0}^{\infty}R^{b}_{n,i} = -k_{p,TDB}P^{=}_{n,i}\lambda^{b}_{0} \quad (2)$$

Here, $\lambda^{b}_{0} = \sum_{n=1}^{\infty}\sum_{i=0}^{\infty}R^{b}_{n,i}$ denotes the zeroth moment of growing chains at the branching catalyst, while $\mu^{=}_{0} = \sum_{n=1}^{\infty}\sum_{i=0}^{\infty}P^{=}_{n,i}$ similarly stands for the zeroth moment of dead chains with a terminal double bond.

Production of chains with a double bond:

$$\frac{dR^{b}_{n,i}}{dt} += k_{p,TDB}\sum_{m=1}^{n-1}\sum_{j=0}^{i-1}R^{b}_{n,i}P^{=}_{n-m,i-j-1} \quad (3)$$

These equations are implemented in the Galerkin FEM code in two ways: the *pseudodistribution* approach[2] and the *classes* approach.[1] We will subsequently discuss these approaches.

Pseudodistributions Model. The 1-dimensional equations describing chain length are obtained from eqs 1, 2, and 3 by summing over number of branches, i:

$$\frac{dR^{b}_{n}}{dt} += k_{p,TDB}R^{b}_{n}\mu^{=}_{0} \quad (4)$$

$$\frac{dP^{=}_{n}}{dt} += k_{p,TDB}P^{=}_{n}\lambda^{b}_{0} \quad (5)$$

$$\frac{dR^{b}_{n}}{dt} += k_{p,TDB}\sum_{m=1}^{n-1}R^{b}_{n}P^{=}_{n-m} \quad (6)$$

The *first* branching moment distribution follows by multiplication of eqs 1, 2, and 3 with the number of branches i and subsequent summation:

$$\frac{d\Phi^{b1}_{n}}{dt} += -k_{p,TDB}\Phi^{b1}_{n}\mu^{=}_{0} \quad (7)$$

$$\frac{d\Psi^{=1}_{n}}{dt} += -k_{p,TDB}\Psi^{=1}_{n}\mu^{b}_{0} \quad (8)$$

The production term as derived from eq 3 requires some more extensive algebraic manipulations:

$$\begin{aligned}
\frac{d\Phi^{b1}_{n}}{dt} &+= -k_{p,TDB}\sum_{i=0}^{\infty}i\Big(\sum_{m=1}^{n-1}\sum_{m=1}^{n-1}R^{b}_{m,j}P^{=}_{n-m,i-j-1}\Big)\\
&= -k_{p,TDB}\sum_{m=1}^{n-1}\sum_{j=0}^{\infty}R^{b}_{m,j}\Big(\sum_{i=j}^{\infty}iP^{=}_{n-m,i-j-1}\Big)\\
&= -k_{p,TDB}\sum_{m=1}^{n-1}\sum_{j=0}^{\infty}R^{b}_{m,j}\Big(\sum_{i=0}^{\infty}(i+j+1)P^{=}_{n-m,i}\Big)\\
&= -k_{p,TDB}\sum_{m=1}^{n-1}\Big(\sum_{j=0}^{\infty}jR^{b}_{m,j}\sum_{i=0}^{\infty}P^{=}_{n-m,i} + \sum_{j=0}^{\infty}R^{b}_{m,j}\sum_{j=0}^{\infty}(i+1)P^{=}_{n-m,i}\Big)\\
&= -k_{p,TDB}\sum_{m=1}^{n-1}(\Phi^{b1}_{m}P^{=}_{n-m} + R^{b}_{m}\Psi^{=1}_{n-m} + R^{b}_{m}P^{=}_{n-m})
\end{aligned} \quad (9)$$

The *second* branching moment distribution follows by multiplication of eqs 1, 2, and 3 with the squared number of branches i^2 and subsequent summation as follows:

$$\frac{d\Phi^{b2}_{n}}{dt} += -k_{p,TDB}\Phi^{b2}_{n}\mu^{=}_{0} \quad (10)$$

$$\frac{d\Psi^{=2}_{n}}{dt} += -k_{p,TDB}\Psi^{=2}_{n}\lambda^{b}_{0} \quad (11)$$

The production term as derived from eq 3 again requires some more extensive algebraic manipulations:

$$\begin{aligned}
\frac{d\Phi^{b2}_{n}}{dt} &+= k_{p,TDB}\sum_{i=0}^{\infty}i^2\Big(\sum_{m=1}^{n-1}\sum_{j=0}^{i-1}R^{b}_{m,j}P^{=}_{n-m,i-j-1}\Big)\\
&= k_{p,TDB}\sum_{m=1}^{n=1}\sum_{j=0}^{\infty}R^{b}_{m,j}\Big(\sum_{i=j}^{\infty-1}i^2P^{=}_{n-m,i-j-1}\Big)\\
&= k_{p,TDB}\sum_{m=1}^{n=1}\sum_{j=0}^{\infty}R^{b}_{m,j}\Big(\sum_{i=0}^{\infty}(i+j+1)^2P^{=}_{n-m,i}\Big)\\
&= k_{p,TDB}\sum_{m=1}^{n=1}\sum_{j=0}^{\infty}j^2R^{b}_{m,j}\sum_{i=0}^{\infty}P^{=}_{n-m,i} +\\
&\quad \sum_{j=0}^{\infty}R^{b}_{m,j}\sum_{j=0}^{\infty}i^2P^{=}_{n-m,i} + 2\sum_{j=0}^{\infty}jR^{b}_{m,j}\sum_{i=0}^{\infty}P^{=}_{n-m,i} +\\
&\quad 2\sum_{j=0}^{\infty}R^{b}_{m,j}\sum_{j=0}^{\infty}i^2P^{=}_{n-m,i} + 2\sum_{j=0}^{\infty}R^{b}_{m,j}\sum_{i=0}^{\infty}P^{=}_{n-m,i} +\\
&\quad \sum_{j=0}^{\infty}R^{b}_{m,j}\sum_{j=0}^{\infty}i^2P^{=}_{n-m,i}\\
&= k_{p,TDB}\sum_{m=1}^{n=1}\Phi^{b2}_{n}P^{=}_{n-m} + R^{b}_{m}\Psi^{=2}_{n-m} +\\
&\quad 2\Phi^{b1}_{m}\Psi^{=1}_{n-m} + 2\Phi^{b1}_{n}P^{=1}_{n-m} + 2R^{b}_{m}\Psi^{=1}_{n-m} +\\
&\quad R^{b}_{m}P^{=}_{n-m}
\end{aligned} \quad (12)$$

The complete overview of population balance equations is given in the Appendix.

Classes Model. Part of the results for the case of pure branching catalyst have been generated using a classes approach similar to that which we have used before.[1] It represents an exact solution of the population balances for a limited chain length. It makes use of the fact that up to this length chains with only few branches are involved. This allows reformulating the population balances by introducing as new reaction "components" separate one-dimensional distribution classes for chains of specific number of branches: $R0_n^b$, $R1_n^b$, $R2_n^b$, etc. for growing chains with 0, 1, 2, etc. branches, and similarly $P0_n^=$, $P1_n^=$, $P2_n^=$, etc. for dead chains (for the pure CGC−Ti case, we do not use more distribution variables). The two-dimensional combination reaction

$$R_{n,i}^b + P_{m,j}^= \xrightarrow{k_{p,TDB}} R_{n+m,i+j}^b$$

is then represented by a series of reactions between the new components of each class:

$$R0_n^b + P0_m^= \xrightarrow{k_{p,TDB}} R1_{n+m}^b$$

$$R1_n^b + P0_m^= \xrightarrow{k_{p,TDB}} R2_{n+m}^b$$

$$R2_n^b + P0_m^= \xrightarrow{k_{p,TDB}} R3_{n+m}^b$$

...

or, in general:

$$RN_n^b + PM_m^= \xrightarrow{k_{p,TDB}} R(N+M+1)_{n+m}^b$$

The size of the problems that can reasonably be handled by the Galerkin FEM code is limited to around 10 classes. If the number of classes is I, then in principle chains with $N + M = I$ are correctly handled. For $N, M \leq I$, the consumption terms in the classes model are correct, but the production terms with $N + M > I$ have to be collected in a sink term. In our classes model, we choose the highest class to serve as a sink. Hence, this class is not correctly dealt with and the highest class that is indeed properly treated is class I-1.

Calculation of Branching Density and Branching Polydispersity in Pseudodistribution Model. The pure CGC−Ti system is described by only two real distribution variables, R_n^b for the growing chains on CGC catalyst and $P_n^=$ for the dead chains (all with a terminal double bond). The branching density for growing and dead chains follows from these distributions and the first branching moment distributions Φ_n^{b1} and $\Psi_n^{=1}$, respectively:

$$b_n^b = \frac{\Phi_n^{b1}}{R_n^b} \; b_n^= = \frac{\Psi_n^{=1}}{P_n^=} \tag{13}$$

The branching polydispersity as a function of chain length for growing and dead chains is based on the second branching moments Φ_n^{b2} and $\Psi_n^{=2}$, respectively:

$$D_n^b = \frac{\Phi_n^{b2}/\Phi_n^{b1}}{\Phi_n^{b1}/R_n^b} \; D_n^= = \frac{\Psi_n^{=2}/\Psi_n^{=1}}{\Psi_n^{=1}/P_n^=} \tag{14}$$

Results

We have performed computations with the classes and pseudodistributions model for single and mixed catalyst systems in CSTR and semibatch reactor. The main part of the kinetic data is taken from previous work on mixed metallocene systems.[7,14] These data, together with reactor data, are listed in Tables 1−3. Figure 1 shows the comparison of MWD from the model with the data from the tables to experimental data for a semibatch reactor with the mixed Et[Ind]$_2$ZrCl$_2$/CGC−Ti system.[7] It further compares the MWDs of experimental work from another source[22] to model predictions for different kinetic assumptions (see caption, Figure 1). For the CSTR, almost good agreement is found, while for the semibatch system discrepancies are somewhat larger. On the basis of Figures1 and 2 we conclude that the coefficients chosen are well within a range to provide reasonable results. Regarding the set of kinetic coefficients as input to the model we decided to adhere to the semibatch based data—despite the larger differences in MWD—since in that case the resulting MWD and branching levels can be consistent with available mixed metallocene MWD/branching data over a whole range of catalyst ratios. Another difference between the two experimental sources[7,22] is the dominant termination mechanism, either β-hydride elemination[7] or transfer to monomer.[22] However, since the effects of both termination mechanisms (both generating chains with un-

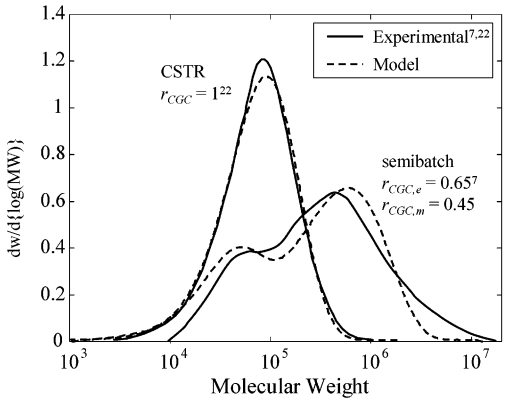

Figure 1. Comparison of molecular weight distribution from model with experiment for CSTR[22] and semibatch reactor.[7] CSTR model: kinetic data of Wang et al.[22] used, $k_{p,CGC}M$ = 5730 s^{-1}, $k_{\beta,CGC}$ = 0.02 s^{-1}, $k_{m,CGC}/k_{p,CGC} = 2.48 \times 10^{-4}$, $k_{p,TDB}$ = 368 m^3/(kmol s), and $k_{H,CGC}$ = 2300 m^3/(kmol s). Effective catalyst concentration (deactivation accounted for): $C_{CGC} = 4.29 \times 10^{-6}$ kmol/m^3. Semibatch model: kinetic data from Table 1.

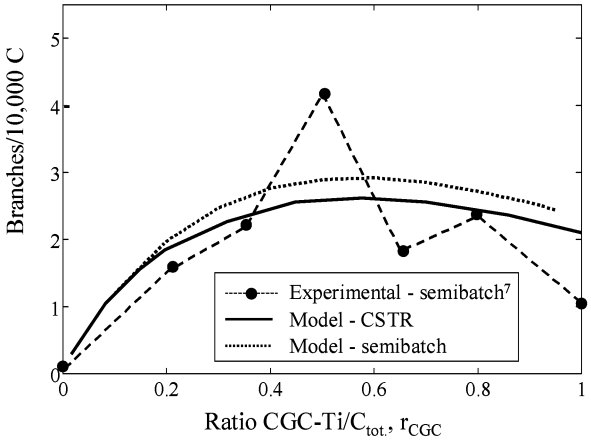

Figure 2. Comparison branching density vs catalyst ratio from model (CSTR and semibatch) to experiment7 for semibatch reactor. Branching densities: 0.35/10 000 C (experiment); 0.36/10 000 C (model). Kinetic data set of Table 1.

Table 2. Standard Values Kinetic Coefficients,[14] Where All Catalyst Deactivation Coefficients Are Assumed To Be Zero

mechanism	rate coeff	value	units
activation CGC−Ti	$k_{i,CGC}/k_{p,CGC}$[a]	1	
activation Et[Ind]$_2$ZrCl$_2$	$k_{i,lin}/k_{p,lin}$[a]	1	
propagation rate CGC−Ti	$k_{p,CGC}$[M][a]	500	s^{-1}
propagation rate Et[Ind]$_2$ZrCl$_2$	$k_{p,lin}$[M][a]	500	s^{-1}
β-hydride elimination CGC−Ti	$k_{\beta,CGC}$	0.3	s^{-1}
β-hydride elimination Et[Ind]$_2$ZrCl$_2$	$k_{\beta,lin}$	0.7	s^{-1}
transfer to monomer CGC−Ti	$k_{m,CGC}/k_{p,CGC}$[a,b]	0	
transfer to monomer Et[Ind]$_2$ZrCl$_2$	$k_{m,lin}/k_{p,lin}$[a,b]	0	
transfer to hydrogen CGC−Ti	$k_{H,CGC}$	250	$[m^3\ kmol^{-1}\ s^{-1}]$
transfer to hydrogen Et[Ind]$_2$ZrCl$_2$	$k_{H,lin}$	0	$[m^3\ kmol^{-1}\ s^{-1}]$
TDB propagation	$k_{p,TDB}$	1750	$[m^3\ kmol^{-1}\ s^{-1}]$

[a] Model does not require separate values for k_p and [M] and rate coefficient ratios for reactions involving monomer; see Appendix. Value for k_p[M] taken from ref 14. Propagation coefficients reported in the literature: k_p = 40 000 m^3/(kmol s),[15] 5700 m^3/(kmol s).[22] [b] Equivalent termination as realized by β-hydride elimination according to $k_{\beta,CGC}$ = 0.3 s^{-1} and $k_{\beta,lin}$ = 0.7 s^{-1} is attained by transfer to monomer for coefficient ratios of 0.006 and 0.014, respectively

Table 3. Simulation Variables

simulation variables	symbol	value	units
volumetric monomer consumption	$(\phi_{M,in} - \phi_{M,out})/V$[a]	0.002	kmol s^{-1} m^{-3}
initial/feed concentration CGC−Ti	$C_{CGC,0}$[b]	$0-4 \times 10^{-6}$	kmol m^{-3}
initial/feed concentration Et[Ind]$_2$ZrCl$_2$	$C_{lin,0}$[b]	$0-4 \times 10^{-6}$	kmol m^{-3}
steady-state concentration CGC−Ti	C_{CGC}	$0-1.2 \times 10^{-8}$	kmol m^{-3}
steady-state concentration Et[Ind]$_2$ZrCl$_2$	C_{lin}	$0-2.8 \times 10^{-8}$	kmol m^{-3}
hydrogen concentration	[H_2]	$0-1.13 \times 10^{-3}$	kmol m^{-3}
batch time		600	s
av residence time CSTR	τ	300	s

[a] In the case of semibatch reactor $-\phi_{M,out} = 0$. [b] Sum of initial catalyst concentrations in all cases equals 4×10^{-6} kmol/m^3.[7]

saturated ends) on MWD and branching are equivalent for proper values of coefficients (see Table 2), the choice for either or both does not influence the MWD/DBD results. Catalyst deactivation is not taken into account in our simulations (Table 3), although our model permits us to do so. We should finally note that in order to perform simulations with the models, we have to choose a kinetic data set. However, the models in themselves are essentially indifferent to such data sets and, in principle, cover all the mechanisms mentioned before.

Comparison of Classes and Pseudodistribution Model. In this paragraph, we present the results for the CSTR case as full bivariate chain length/number of branch points distributions. We compare the molecular weight and branching density distributions to those obtained with the pseudodistributions model. Furthermore, in the next paragraph we employ the results from the classes model to examine the statistics of the chains with various numbers of branch points. We will do this both for the CSTR and for the semibatch reactor.

Pure CGC−Ti Case in CSTR. The full bivariate chain length-number of branches distribution obtained from a classes model with nine classes for the case of pure CGC−Ti in a CSTR is given in Figure 3a. This is the simplest case, since one catalyst is involved, producing TDB chains only, under steady-state conditions. These results, identical for growing and dead chains, are valid for chains with up to seven branches (the eighth class collects all the chains yielding eight or more branches). This becomes clear when comparing the average number of branches vs chain length from the classes model to the pseudodistribution model, as from Figure 4. It turns out that the chain length validity limit of the classes model lies at around 10 000. Until this limit the average branching numbers from the classes and pseudodistribution models coincide. This is not surprising, since the models contain the same assumptions and neither of them requires extra assumptions or closure relations. The equivalence of both models

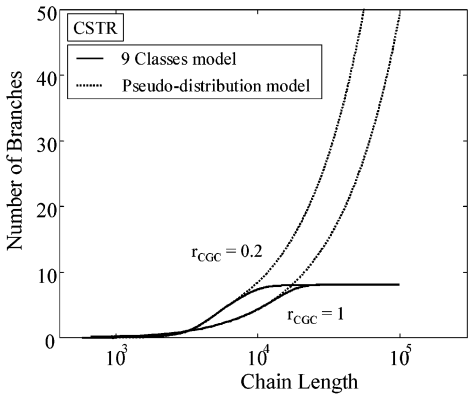

Figure 3. Average number of branches vs chain length from the nine-classes and pseudodistributions models, dead chains, CSTR case. For pure branching catalyst system, $r_{CGC} = 1$, and for the mixed system, $r_{CGC} = 0.2$. Maximum number of branches in the nine-classes model equals 8. For $r_{CGC} = 1$, identical plots for living and dead chains are found.

holds as well for the branching density as a function of chain length and the chain length distributions. Note besides that the plots are identical for growing and dead chains, since the dead chains are being produced by a transfer reaction from just one population of growing chains and are not modified by that reaction. For this one-catalyst/CSTR case, an analytical expression has been derived[4] containing one kinetic parameter for the bivariate chain length/number of branches distribution. We have compared our results to the outcomes from the analytical solution and found exact agreement.

Mixed Catalysts in CSTR. Calculations have been performed using the nine-classes model for the mixed catalyst system, with catalyst ratio (defined as the molar fraction of branching catalyst in the total amount of catalyst) $r_{CGC} = 0.2$. The resulting bivariate chain length/number of branch points distribution is shown in Figure 3b. The most remarkable difference with the single catalyst system is the existence of relatively high

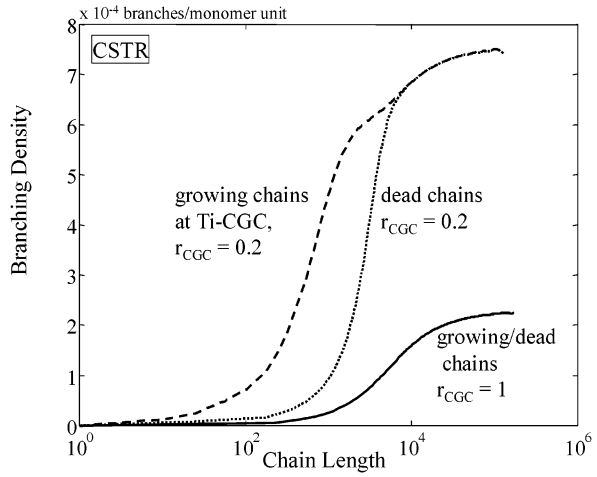

Figure 4. Branching density vs chain length from pseudo-distribution model for pure branching catalyst ($r_{CGC} = 1$) and mixed catalyst ($r_{CGC} = 0.2$) system, CSTR case. Plots were identical for living and dead chains in the case of $r_{CGC} = 1$. Branching density of dead chains is lower at smaller chain lengths since this population includes the (shorter) chains produced at the nonbranching catalyst.

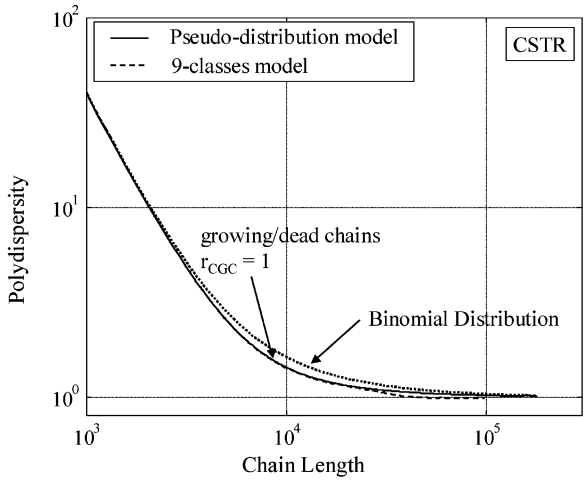

Figure 6. Polydispersity vs chain length for pure branching catalyst ($r_{CGC} = 1$) from the nine-classes and pseudodistribution models, CSTR case. Results of models coincide until validity limit of classes model, $n = 10\,000$. Both models predict smaller polydispersity than binomial branching distribution at intermediate chain lengths.

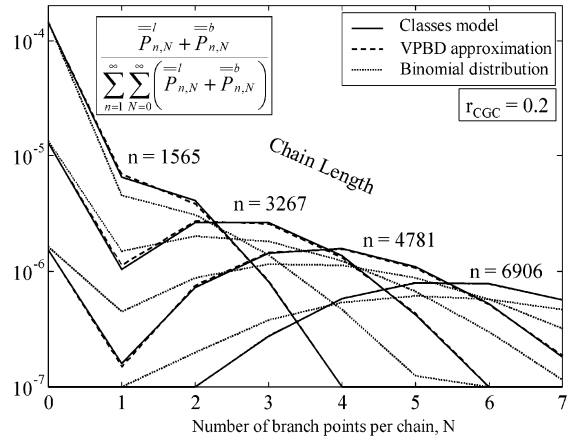

Figure 5. Fractional distribution of chains from both catalysts over number of branch points N for various chain length, n, calculated exactly from the nine-classes model (drawn curve), BD approximation (dotted curve), and VPBD (broken curve) approximation, catalyst ratio $r_{CGC} = 0.2$. Exact distributions of dead chains from CGC−Ti (all chains with $N \geq 1$) from classes model narrower than BD approximation. An almost perfect agreement between VPBD approximation and exact solution is seen. The presence of high concentration of branchless chains from Et[Ind]$_2$ZrCl$_2$ catalyst is clearly visible as a peak at $N = 0$.

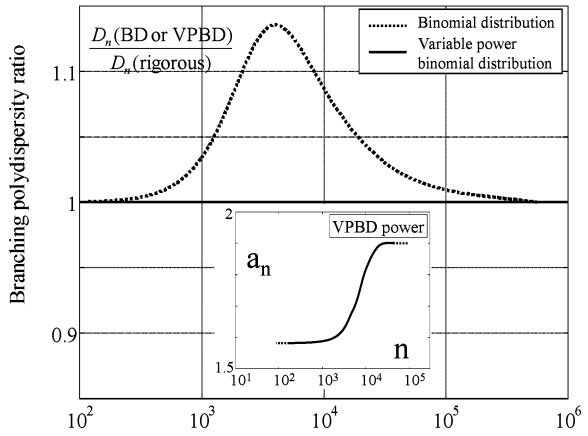

Figure 7. Ratio of branching polydispersity (upper graph) calculated assuming binomial distribution shape (BD, broken curve) and variable power binomial distribution (VPBD, drawn curve, eq 17) to polydispersity from rigorous distribution, vs chain length. BD solution overestimates D_n by almost 15% at $n = 5000$. Power a_n as a function of chain length (lower-left) calculated from Galerkin pseudodistribution model. At lower and higher chain lengths, small computational errors in the polydispersity prevent an accurate fit of a_n; in these ranges, the BD solution is valid. Absolute polydispersities are depicted in lower-right curve, where VPBD and rigorous solution coincide.

concentrations of branchless chains, appearing as a ridge at $N = 0$. (This is even more visible in a number of branch point distributions at constant chain length in Figure 7b.) This is obviously due to the contribution of the Et[Ind]$_2$ZrCl$_2$ catalyst to the branchless chains production. This time the validity of the nine-classes model runs to chain lengths of around 5000. Until this length the pseudodistribution model coincides with the nine-classes model. Note that no other reference for comparison is available for the bivariate chain length/number of branches distribution regarding this mixed catalyst system, since the analytical solution mentioned before[4] only holds for a single catalyst system.

Chain Statistics, Branching Density, and Branching Polydispersity. Populations of All Chains. On the basis of the results from the nine-classes model, we will now discuss chain statistics in general. In particular, we will relate this discussion to what we observe regarding branching density and branching polydispersity as a function of chain length. First, we check the statistical properties of the chains. In the presence of only one catalyst one would expect chain growth to be governed by the relative probability of propagation, β-hydride elimination, and insertion of a chain with a TDB. This would imply that the average length of all branchless chains and chain segments between branch points or between a branch point and a chain end point, $\bar{s}_n$, is equal. Note that for a CSTR $\bar{s}_n$ assumes its steady-state value, while in a semibatch reactor this argument holds for the instantaneous average chain length $\bar{s}_n$ (value for dead chains created at a certain time instant). The (instantaneous) segment length distribution should then possess a Flory shape. We can check this by calculating the number-average segment lengths for all

the chains with different numbers of branch points from the classes model. Indeed, the average (instantaneous) segment length turns out to be independent of the number of branch points on a chain, always obeying

$$\bar{s}_n = \frac{k_p M}{k_p M + k_\beta + k_{p,TDB}\mu_0^{=}} \tag{15}$$

In the CSTR case, the value turns out to equal $\bar{s}_n = 995$. This result also implies, for the CSTR, that all monomer units in chains have an equal probability of being branched. In this respect one concludes that in this single catalyst CSTR system all the chains obey the same statistics, as has been recognized before.[6] In the mixed catalyst system, the statistical equality of all chains no longer holds true. Here are two catalyst systems active with different growth statistics. The population of chains without branches is now a mixed product of two catalysts. We see this confirmed by Figure 5a, which displays the average segment length as a function of number of branches on the chain, for a CSTR. In this case, the branchless chains are longest, chains with $N = 1$ shortest, while the average length steadily increases from $N > 1$. Hence, we conclude that in the complete population of chains in the mixed catalyst CSTR system chains possess different statistics. Finally, in a semibatch reactor chain statistics should be explored in relation to possible variations over time. Note that the argument on the average, $\bar{s}_n$, holds for the instantaneous chain length. Applying the classes model to the semibatch reactor for the single CGC−Ti catalyst case, we calculated $\bar{s}_n$ for all chains with different numbers of branches as a function of time and we found the profiles as depicted in Figure 5b. Now, we observe both differences between chains having different numbers of branches, in contrast to the CSTR single catalyst system, as well as $\bar{s}_n$ changing with time. The latter phenomenon is obviously connected to the increase of the polymer concentration $\mu_0^{=}$ over time, which according to eq 9 leads to lower $\bar{s}_n$. This is also in agreement to the increase of branching density over time. The fact that chains with more branches possess the longer average segment lengths can be explained as follows. Chains with branches are created by insertion, in actually growing chains, of older (branched) chains created at an earlier stage in the batch. The more branches a molecule carries, the higher the content of relatively old parts being created at early stages, during which the average segment length is higher. In conclusion, we observe that in a semibatch reactor the statistics of chains are different, depending both on the instant during the batch they are created and on the number of branches they carry. This will become important when constructing architectures from the molecular weight and branching data as generated. Doing this, one has to account for chain length, degree of branching, and time of creation, so ultimately the bivariate chain length/degree of branching distributions are required at several time instants during the batch. By a similar argument, it is evident that attributing rheological properties to segments, as has been performed for a single catalyst CSTR case under the assumption of identical statistics of all chains,[6] is not directly applicable on either a CSTR with mixed catalysts or any semibatch reactor system. In the semibatch case, this would require an architectural resolution down to the full bivariate *n*, *N* distribution at several time instants.

Populations at Given Chain Length. Next we regard the statistics of chains at a given chain length rather than whole populations of chains. This is relevant in obtaining the full bivariate chain length-number of branches distribution from the pseudodistribution model. The nine-classes model directly provides us with this bivariate distribution, but only to chain lengths up to 10 000. Generating this distribution for the whole relevant chain length range from the pseudodistribution model requires the monovariate chain length distribution and average degree of branching distributions as calculated from that model. The issue is then that construction of branching distributions at each chain length requires making an assumption about the shape of the branching distribution. Supposing that each monomer unit in a chain of given length has equal probability of being branched suggests that the branching distribution can be described by a *binomial distribution*.

As regards branching density vs chain length, we see the result for a CSTR in Figure 4. Branching density increases with chain length. This reflects the kinetic fact that shorter chain lengths are more probably generated by propagation only than by propagation and subsequent TDB insertion. In this region, chains carry less than one branch point on average. For the single ($r_{CGC} = 1$) and mixed catalyst ($r_{CGC} = 0.2$) cases the number of branch points distributions are given for various (dead) chain lengths in Figure 5. Here, we compare the branching distributions from the exact solution of the classes model to those calculated from the branching density and assuming a binomial distribution. Note that for mixed catalyst systems more than one option is available to do so, since the dead chain distribution is composed of two sub-populations: chains originating from CGC−Ti ($P_n^{b=}$) and from Et[Ind]$_2$ZrCl$_2$ ($P_n^{l=}$). We will employ the following two options. The first possibility is assuming a binomial shape for the branching distribution of the *whole population* of dead chains. The second option is to apply the binomial shape on the populations of dead chains from *CGC−Ti only*. Our model allows distinguishing between $P_n^{b=}$ and $P_n^{l=}$ as described in the Appendix (eqs 10 and 11). Thus, to construct the bivariate chain length/number of branch points distribution for the whole dead chain population after the second option, we first compute the bivariate distribution $P_{n,i}^{b=}$ for the dead chains from CGC−Ti, and then we add the linear distribution: $P_{n,0}^{=} = P_{n,0}^{b=} + P_n^{l=}$. In this way the binomial approximation of Figure 5 for a mixed catalyst system was constructed. We observe, for all catalyst ratios, that the exact distribution for dead chains from the branching catalyst is *narrower* than a binomial distribution. This is confirmed by comparing the branching polydispersity vs chain length curves for the binomial and exact distributions, as shown for $r_{CGC} = 1$ in Figures 6 and 7. For short and long chains, the branching distribution polydispersity accords to the binomial values, but at intermediate chain length it is slightly, but significantly, smaller.

In view of these discrepancies, we should find an alternative approximation method that generates branching distributions at a given chain length with correct values for both the average number of branch points $\bar{N}_n$ *and* the branching polydispersity D_n. For the binomial distribution (eq 17, with $a = 1$) these quantities

directly follow from well-known moment equations:[27]

$$\bar{N}_n = \rho_n \quad \text{and} \quad D_n = (1 - \rho + \bar{N}_n)/\bar{N}_n \qquad (16)$$

These expressions in principle allow calculating, at each chain length n, a parameter set n' and ρ' yielding the correct pair of $\bar{N}_n$ and D_n. However, especially at the lower chain length range, this leads to n' values near 1, obviously nondiscrete. Now, the binomial distribution does require discrete n', hence no such distribution exists that exactly can generate the desired $\bar{N}_n$ and D_n. A continuous variant of the binomial distribution allowing broken numbers for the parameter n' did not work in a straightforward way either, since the moment expressions for the discrete variant do not apply to the continuous one. Several other standard discrete distributions were tested, but none could satisfy the demand. Therefore, we decided to employ a three-parameter binomial distribution with a modification being the raising of it to a power a_n (the third parameter) varying with chain length, the variable power binomial distribution (VPBD):

$$p_{n,N} = \left\{ \binom{n}{N} (\rho_N)^N (1 - \rho_n)^{(n-N)} \right\}^{a_n} \qquad (17)$$

An average number of branch points and polydispersity can be obtained from the VPBD as follows:

$$\bar{N}'_n = \frac{\sum_{N=0}^{\infty} N p_{n,N}}{\sum_{N=0}^{\infty} p_{n,N}} \quad D'_n = \frac{\sum_{N=0}^{\infty} N^2 p_{n,N}}{\sum_{N=0}^{\infty} N p_{n,N}} \Bigg/ \frac{\sum_{N=0}^{\infty} N p_{n,N}}{\sum_{N=0}^{\infty} p_{n,N}} \qquad (18)$$

Now, only for $a = 1$ this returns the correct value for the average number of branch points $\bar{N}_n$, but for other values, this does not hold true. Note that in the VPBD the parameter a permits to change distribution width: $a > 1$ leads to a narrower distribution. The fitting procedure at specific n varies a_n, each value yielding a specific pair of n' and ρ' that satisfies $n'\rho' = \bar{N}_n$ and provides a specific D_n value. Finding D_n as predicted by the Galerkin−FEM pseudodistribution method is then the target of the a_n-variation. The results of the VPBD approximation are satisfactory. Figure 7 (inset) shows that the variable power a_n indeed has values larger than one, leading to narrowing of the distribution. At lower and higher chain lengths small computational errors in the polydispersity prevent an accurate fit of a_n; note that in these ranges the BD solution is valid.

A perfect fit is obtained for branching polydispersity (Figures 6 and 7), while the VPBD branching distributions at fixed n (Figure 5) practically coincide with the classes model. For $r_{CGC} = 1$ the VPBD solution turns equally out to coincide with the analytical solution.[4]

Simulations at Varying Catalyst Ratio. In this part, the effect of the catalyst ratio on the molecular weight, branching density, and polydispersity will be addressed for the CSTR and semibatch reactor case, in the absence and presence of hydrogen. In addition, some results on the dynamics of these quantities in the semibatch system will be presented.

Absence of Hydrogen. In Figure 8, the molecular weight distributions of the CSTR and semibatch reactor are compared under various catalyst ratios. Bimodalities are clearly present and completely vanish only in the single catalyst systems. One observes a remarkable similarity between the two reactor systems, the bimodality appearing almost equally strong in the CSTR. This must be attributed to the persistence, in the CSTR, of the effect observed in the semibatch reactor of two catalysts producing polymer under highly different conditions. The quantitative proportions of the products formed in the CSTR are apparently similar, since the average residence time is sufficient for the "slower" branching catalyst to produce polymer in significant amounts. Note in this respect that indeed the polymerization process at the CGC−Ti has slow elements: the formation of branches. This will become more apparent when addressing the dynamics of the system, hereafter (Figure 10).

As regards overall reactor average branching density $\bar{\rho}_b$ in function of catalyst ratio, Figure 2 shows that the CSTR features a similar maximum as the semibatch reactor, at a slightly lower level. Note that this maximum in branching density could also be found by a much simpler model.[23] The level of average branching density at each chain length, ρ_b, shows a steady *increase*

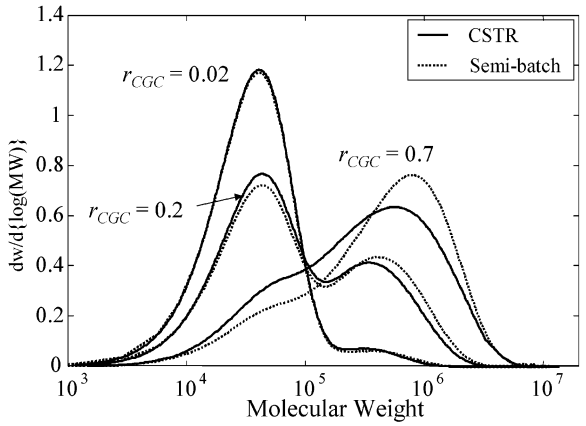

Figure 8. Molecular weight distributions for various catalyst ratios for semibatch reactor (a) and CSTR (b), no hydrogen. CSTR features bimodality as well, and the shape difference increases with branching catalyst content. Note that these MWDs result from the superposition of two dead chain distributions having identical shape: $P_n^{=} = P_n^{b=} + P_n^{l=}$ (Appendix).

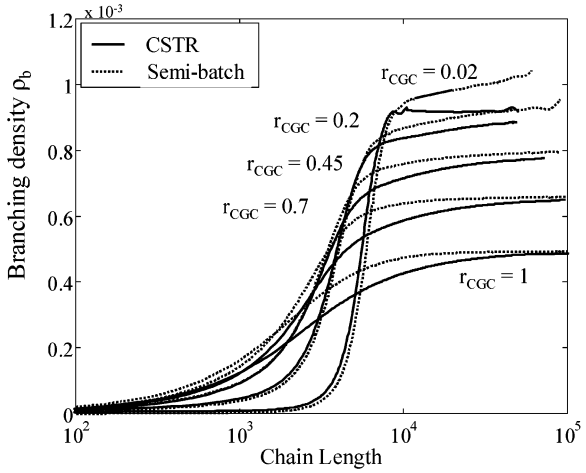

Figure 9. Branching density vs chain length for various catalyst ratios, CSTR, and semibatch reactor case. The highest branching density is observed on long chains at low catalyst ratio (lowest overall average branching density, see Figure 2). No hydrogen.

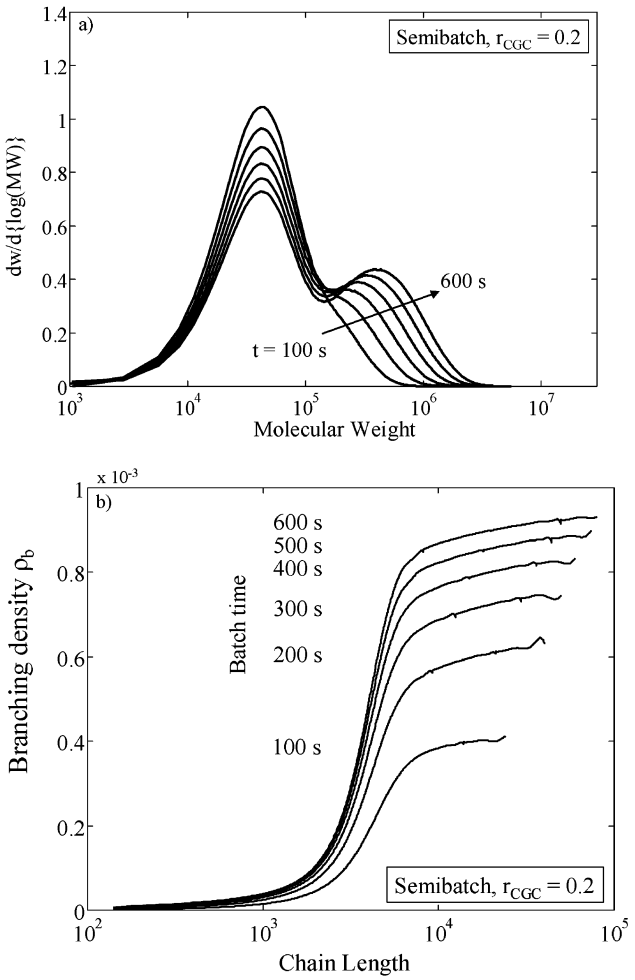

Figure 10. Development of molecular weight distribution (a) and branching density (b) over time in a semibatch reactor. MWD bimodality appears at later stages.

as branching catalyst content, r_{CGC}, decreases, as goes from Figure 9. This is still consistent with the lower overall branching density average at low r_{CGC}, as we realize that only a minor part of the chains possess lengths and branching densities at such levels. This becomes apparent by regarding the MWDs of Figures 8.

The dynamics of chain length and branching distributions in a semibatch reactor is illustrated in Figure 10. As regards molecular weight distribution (Figure 10a), one observes that it takes the whole batch time for the high MW peak to develop, while the low MW peak appears practically instantaneously. This indicates that chain growth through branch formation is a relatively slow process. Figure 10b shows the development of the branching density distribution, steadily increasing with time.

Presence of Hydrogen. Calculations have been performed for a hydrogen content of 1.13×10^{-3} kmol/m^3. Transfer to hydrogen reaction implies the production of dead chains without a terminal double bond. Obviously, this must have significant effects, since dead chains produced by this transfer reaction are not inserted in growing chains at the CGC−Ti catalyst. The resulting molecular weight distributions for both the chains without and with TDB are shown in Figure 11. Chains without TDB are longer on average, since they are made at the branching catalyst only, which creates

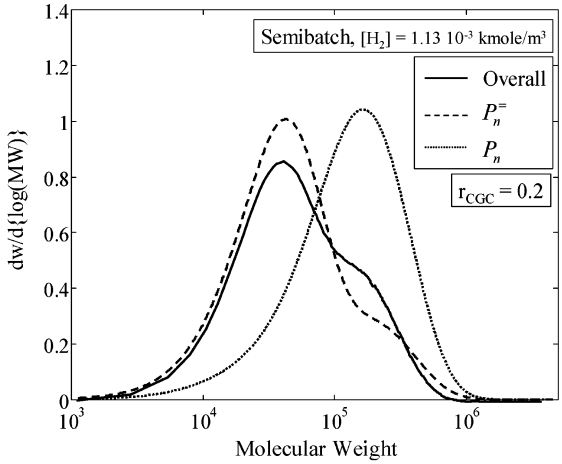

Figure 11. Molecular weight distributions of chains without terminal double bond, Pn (from CGC−Ti only) and with terminal double bonds, $P_n^{=}$(superposition of distributions $P_n^{b=}$and $P_n^{l=}$); semibatch case, catalyst ratio $r_{CGC} = 0.2$, $[H_2] = 1.13 \times 10^{-3}$ kmol/m^3. Two chain types are clearly different. Chains without TDB are longer, being made by transfer to hydrogen at CGC−Ti catalyst only. Together, distributions produce a bimodal overall distribution.

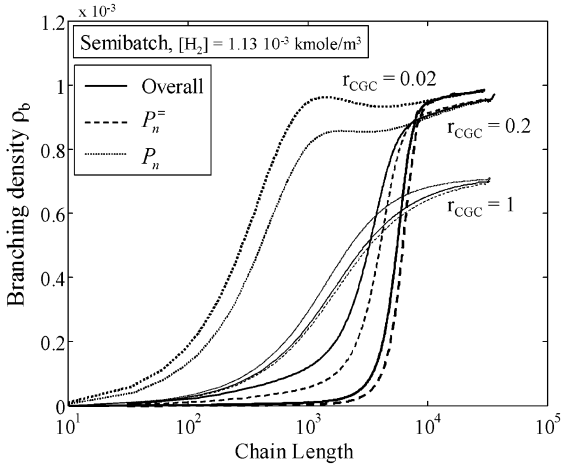

Figure 12. Branching density distributions of chains without, P_n, and with terminal double bonds, $P_n^{=}$, for various catalyst ratios r_{CGC}: semibatch case, $[H_2] = 1.13 \times 10^{-3}$ kmol/m^3. In the case of only branching catalyst, $r_{CGC} = 1$, branching curves are similar, since both chain types are produced at one catalyst. For mixed catalyst systems curves are different. Chains without TDB, P_n, only made by CGC−Ti, have higher branching density in the shorter chain length region, where the curve for $P_n^{l=}$ represents an average of branched and nonbranched chains.

branched and hence long chains. In contrast, chains with TDB are also produced as linear chains at the nonbranching catalyst, and are therefore shorter. Both distributions together yield a bimodal distribution. Results concerning branching density distribution on chains without and with TDB are shown in Figure 12. In the case of only a branching catalyst, minor differences are observed, since all the chains are produced under the same circumstances at one catalyst. Mixed catalyst systems yield clear differences between the two chain types. Those without TDB are assumed to be produced at CGC−Ti only and therefore possess a higher branching density. The curves representing chains with TDBs represent a collection of chains produced at both catalyst, among which a significant

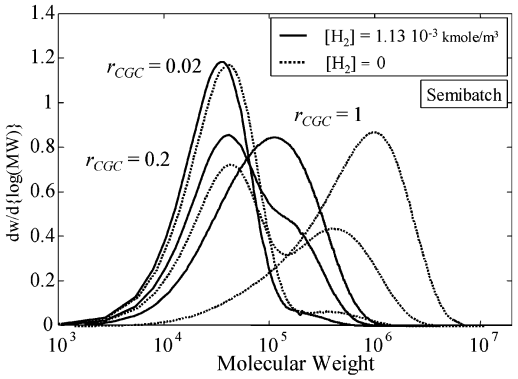

Figure 13. Narrowing effect of hydrogen on mol wt distribution for various catalyst ratios r_{CGC}: semibatch case.

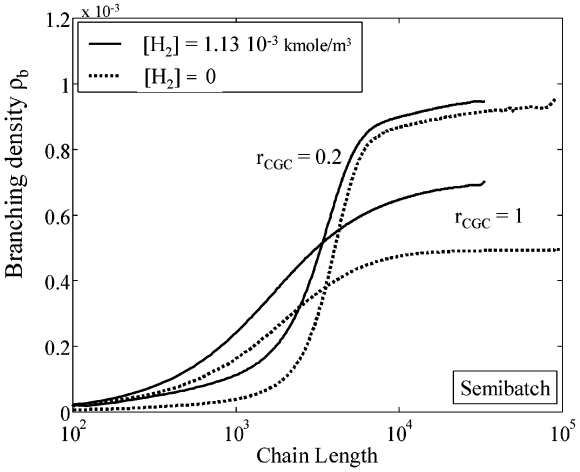

Figure 14. Effect of hydrogen on branching density distribution for catalyst ratio r_{CGC}: semibatch case. For both catalyst ratios the curves are at a higher level due to hydrogen. Note that the average branching density ($\bar{\rho}_b \approx 4 \times 10^{-4}$, see Figure 2) is not influenced by hydrogen.

part nonbranched, hence a lower branching density level.

Figure 13 shows the effect of hydrogen addition on the molecular weight distributions at various catalyst ratios for the semibatch reactor. The CSTR shows similar behavior (not shown). One sees a strong narrowing effect due the presence of hydrogen. The hydrogen effect on branching density distribution in a semibatch reactor is depicted in Figure 14. Interestingly, we see the branching density level to increase due to hydrogen (also for the CSTR). This is not in contrast to the fact that the overall average reactor branching density is not affected by hydrogen. Although the branching density may be higher for all chain lengths, the overall average also depends on the relative numbers of chains having these branching densities. One should realize that in the presence of hydrogen concentrations of chains with shorter length are higher, which possess the lower branching density.

Finally, the full bivariate chain length/number of branch points distribution is given in Figure 15, for the case of a CSTR, with a catalyst ratio $r_{CGC} = 0.2$, in the presence of hydrogen at a concentration of 1.13×10^{-3} kmol/m^3. The bivariate distribution has been derived from the monovariate molecular weight and branching density distributions. To construct it, we approximated the branching distribution of the dead chains from CGC−Ti at each chain length with a variable power binomial distribution. The power a_n as varying with

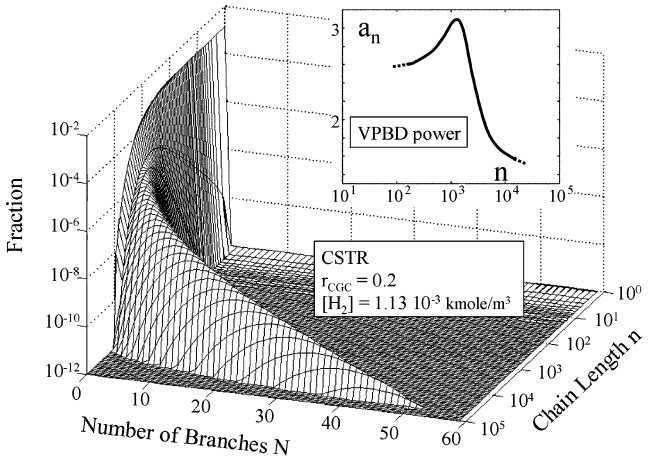

Figure 15. Bivariate chain length/number of branches distribution, CSTR case, mixed catalysts, $r_{CGC} = 0.2$, hydrogen present, on the basis of molecular weight distribution and branching distribution from the Galerkin FEM model. Assumption: variable power binomial distribution (eq 17) of number of branch points at each chain length of dead chains from CGC−Ti with power a_n as shown in the inset (again limited accuracy at lower and higher chain lengths, cf. Figure 7). The discontinuity at $N = 1$ indicates the existence of a "ridge" at $N = 0$, due to the contribution of branchless chains from $Et[Ind]_2ZrCl_2$.

chain length n (inset in Figure 15) was obtained from the branching polydispersity as computed from the Galerkin pseudodistribution model. The bivariate distribution correctly shows the higher concentration of branchless chains originating from linear catalyst, visible as a discontinuity in the distribution at $N = 1$.

Conclusions

We have addressed the problem of finding the bivariate chain length/number of branch points distribution for polyethylene produced by a mixed metallocene catalyst system in continuous and semibatch reactors in two ways. In the first method, we defined distinct classes of chains with a certain number of branches and solved this problem with the Galerkin FEM approach of PREDICI. Employing a model with nine classes we directly found the exact, full bivariate distribution, but only up to chains with seven branches and lengths until around 10 000. According to the second approach, we calculate the monovariate chain length and branching density distribution, the latter using the pseudodistribution method.[2] This method allows calculating the first and second branching moment as a function of chain length, from which the branching density and branching polydispersity at each chain length, respectively, can be derived. The classes and pseudodistribution models yield identical results up to the validity limit of the former. This is attributed to the fact that both models are exact in the sense that no additional assumptions or closure relations are necessary. Moreover, these results coincide with that from an analytical solution for the case of a single catalyst in a CSTR.[4]

Computing the monovariate chain length and branching distributions is not a goal in itself. It serves to constructing molecular architectures, from which radius of gyration distributions or rheological properties can be derived. In general, inferring architectures or architectural properties in relation to, e.g., rheology[6] requires additional information concerning chain statistics—that is, the manner in which several parts of molecules are

connected. We tested the statistical properties of chains for single and mixed metallocene systems in CSTR and semibatch reactor by calculating the average segment lengths. Segments are branchless chains, free-dangling ends and interbranch segments. In a single catalyst CSTR system all of these turned out to have identical lengths, since they are determined by the relative rates of all kinetic mechanisms involved of just one catalyst, rates being constant in a CSTR. This is in line with the fact that any monomer unit in a whole CSTR population of chains has equal probability of being branched. It also confirms the validity of the assumption as it was made for the CSTR/single catalyst system in a study of rheological properties of branched architectures.[6] For the mixed system in a CSTR, from calculations with the classes model, we concluded that the statistical equality no longer holds, since processes at two catalysts co-determine statistical properties. In a semibatch reactor chains were found to be statistically different even for a single CGC−Ti system. Because of increased polymer concentration the average segment length becomes smaller. Moreover, chains with more branches possess the longer average segment lengths. Hence, for future construction of architectures in a semibatch reactor the full n,N distributions at several time instants are needed, since these contain the statistical information minimally required to perform such a task. A related question is concerned with the shape of the branching distribution at fixed chain length. This question needs to be answered when constructing the full n,N distributions from monovariate chain length and branching density distributions as going from the pseudodistribution model. Assuming equal probability of being branched for each monomer unit in chains of a certain length implies that the number of branch points would obey a binomial distribution at each chain length. We calculated the branching polydispersity as a function of chain length from both the classes and the pseudodistribution model. For growing chains at the branching catalyst in single and mixed catalyst systems in CSTR and semibatch reactor, we always found the branching distribution to be *narrower* than that of the binomial distribution. We noticed that branching density was well reproduced, but branching polydispersity was not. Therefore, we constructed an alternative distribution, the variable power binomial distribution (VPBD), having one extra parameter (power a_n) to obtain the correct branching polydispersity as prescribed by the pseudodistribution or classes model. The VPBD method yields almost perfect fits to polydispersities and branching distributions.

The pseudodistribution model allowed us to perform a number of sensitivity calculations for both reactor systems under varying conditions, including dynamics of MWD, DBD, and branching polydispersity in a semibatch reactor. We explored the effect of catalyst ratio and hydrogen addition only, but to this a whole range of kinetic effects can be added to this, like catalyst deactivation. It is interesting to see that the remarkable bimodality in the molecular weight distribution at catalyst ratios of around 0.5 observed in the semibatch system,[7] persists in the CSTR. Equally, a maximum in overall branching density is found for such a ratio in the CSTR. Addition of hydrogen leads to narrowing of the MWD in both reactor systems, as observed before for the semibatch system. The level of the branching density turns out to shift upward. This is still in line with the unchanged overall branching density, since the branching density strongly increases with chain length, while hydrogen leads to higher concentrations of short chains with fewer branches.

Finally, we present the full bivariate chain length/number of branch points distribution as obtained from the pseudodistribution model for the case of a mixed catalyst system in a CSTR with hydrogen addition. As regards branching distribution shape, we applied the VPBD method. In future, we will construct molecular architectures on the basis of both the binomial and variable power binomial distribution to test the validity of these approximations.

Nomenclature

$R^{\mathrm{b}}_{n,i}$ = polymer growing on CGC−Ti catalyst
R^{l}_{n} = polymer growing on linear catalyst (0 branches)
$P^{\mathrm{b=}}_{n,i}$, $P^{\mathrm{l=}}_{n,0}$, $P^{=}_{n,i}$ = dead polymer with terminal double bond from CGC−Ti, $\mathrm{Et[Ind]_2ZrCl_2}$ and their sum, respectively
$P^{\mathrm{b}}_{n,i}$, $P^{\mathrm{l}}_{n,0}$, $P_{n,i}$ = dead polymer without terminal double bond from CGC−Ti, $\mathrm{Et[Ind]_2ZrCl_2}$ and their sum, respectively
$\mu^{=}_{0} = \sum_{\mathrm{n}=1}^{\infty}\sum_{\mathrm{i}=0}^{\infty}$
$P^{=}_{n,i}\mu_0 = \sum_{\mathrm{n}=1}^{\infty}\sum_{\mathrm{i}=0}^{\infty} P_{n,i}$
$\lambda^{\mathrm{b}}_{0} = \sum_{\mathrm{n}=1}^{\infty}\sum_{\mathrm{i}=0}^{\infty}$
$R^{\mathrm{b}}_{n,i}\lambda^{\mathrm{l}}_{0} = \sum_{\mathrm{n}=1}^{\infty} R^{\mathrm{l}}_{n}$
$R^{\mathrm{b}}_{n} = \sum_{\mathrm{n}=1}^{\infty} R^{\mathrm{b}}_{n,i}$
$P^{\mathrm{b=}}_{n} = \sum_{\mathrm{i}=0}^{\infty}$
$P^{\mathrm{b=}}_{n,i}P^{\mathrm{l=}}_{n} =$
$P^{\mathrm{l=}}_{n,0}P^{=}_{n} = \sum_{\mathrm{i}=0}^{\infty} P^{=}_{n,i}$
$P^{\mathrm{b}}_{n} = \sum_{\mathrm{i}=0}^{\infty}$
$P^{\mathrm{b}}_{n,i}P^{\mathrm{l}}_{n} =$
$P^{\mathrm{l}}_{n,0}P_{n} = \sum_{\mathrm{i}=0}^{\infty} P_{n,i}$
$\Phi^{\mathrm{b1}}_{n} = \sum_{\mathrm{i}=0}^{\infty} iR^{\mathrm{b}}_{n,i}$
$\Psi^{=1}_{\mathrm{n}} = \sum_{\mathrm{i}=0}^{\infty} i$
$P^{=}_{n,i}\Psi^{1}_{\mathrm{n}} = \sum_{\mathrm{i}=0}^{\infty} iP_{n,i}$
$\Phi^{\mathrm{b2}}_{n} = \sum_{\mathrm{i}=0}^{\infty} i^2R^{\mathrm{b}}_{n,i}$
$\Psi^{=2}_{n} = \sum_{\mathrm{i}=0}^{\infty} i^2$
$P^{=}_{n,i}\Psi^{2}_{\mathrm{n}} = \sum_{\mathrm{i}=0}^{\infty} i^2P_{n,i}$

Appendix

We here present a full overview of all the equations in the model, per low- or high-molecular species involved. They are valid for a batch reactor. In the case of a CSTR the rhs of the expressions contains an extra term $(c_0 - c)/\tau$, where c_0 is the species feed concentration (nonzero if present in the feed) and τ is the average residence time. The situation is different for the monomer, as will be explained after presenting the equations.

Balance of catalysts

$$\frac{\mathrm{d}C^{*}_{\mathrm{CGC}}}{\mathrm{d}t} = k_{\mathrm{a,CGC}}C_{\mathrm{CGC}} - k_{i,\mathrm{CGC}}MC^{*}_{\mathrm{CGC}} + (k_{\beta,\mathrm{CGC}} + k_{\mathrm{m,CGC}}M + k_{\mathrm{H,CGC}}H_2)\lambda^{\mathrm{b}}_{0} - k_{\mathrm{d2,CGC}}C^{*}_{\mathrm{CGC}} \quad \text{(A1)}$$

$$\frac{\mathrm{d}C^{*}_{\mathrm{lin}}}{\mathrm{d}t} = k_{\mathrm{a,lin}}C_{\mathrm{lin}} - k_{i,\mathrm{lin}}MC^{*}_{\mathrm{lin}} + (k_{\beta,\mathrm{lin}} + k_{\mathrm{m,lin}}M + k_{\mathrm{H,lin}}H_2)\lambda_0{}^{\mathrm{l}} - k_{\mathrm{d2,lin}}C^{*}_{\mathrm{lin}} \quad \text{(A2)}$$

Here, $\lambda^{\mathrm{l}}_{0} = \sum_{n=1}^{\infty}\sum_{i=0}^{\infty} R^{\mathrm{l}}_{n,i}$ denotes the zeroth moment of growing chains at the linear catalyst. We assume the activation rate coefficients to be very high (instantaneous activation) so that eqs A1 and A2 can be solved

with the initial catalyst concentrations as the starting values for the activated catalyst concentrations C^*_{lin} and C^*_{CGC}.

Monomer balance

$$\frac{dM}{dt} = -\{k_{i,lin}C^*_{lin} + k_{i,CGC}C^*_{CGC} + (k_{p,lin} + k_{m,lin})\lambda^b_0 + (k_{p,CGC} + k_{m,CGC})\lambda^l_0\}M \quad \text{(A3)}$$

Population balances of growing chains at both catalysts and polymer chains without and with terminal double bond.

In the full 2 dimensions:

$$\frac{dR^l_{n,0}}{dt} = k_{i,lin}MC^*_{lin}\delta(n-1) + k_{p,lin}([R^l_{n-1,0} - R^l_{n,0})M - (k_{\beta,lin} + k_{d1,lin} + k_{m,lin}M + k_{H,lin}H_2)R^l_{n,0} \quad \text{(A4)}$$

Here δ(i) is the Kronecker's δ function which has a value of 1 for $i = 0$ and a value of 0 for i $\neq$ 0. Note that growing chains at the linear catalyst do not carry branches; hence, the second index is always zero.

$$\frac{dR^b_{n,i}}{dt} = k_{i,CGC}MC^*_{CGC}\delta(n-1) + k_{p,CGC}(R^b_{n-1} - R^b_n)M - (k_{\beta,CGC} + k_{d1,CGC} + k_{m,CGC}M + k_{H,CGC}H_2)R^b_{n,i} + k_{p,TDB}(-\mu^{=}_0 R^b_{n,i} + \sum_{m=1}^{n-1}\sum_{j=0}^{i} P^{=}_{m,j}R^b_{n-m,i-j-1}) \quad \text{(A5)}$$

$$\frac{dP^{l=}_{n,0}}{dt} = (k_{m,lin}M + k_{\beta,lin} + k_{d1,lin})R^l_{n,0} - k_{p,TDB}P^{l=}_{n,0}\lambda^b_0 \quad \text{(A6a)}$$

$$\frac{dP^{b=}_{n,i}}{dt} = (k_{m,lCGC}M + k_{\beta,CGC} + k_{d1,CGC})R^b_{n,i} - k_{p,TDB}P^{b=}_{n,i}\lambda^b_0 \quad \text{(A6b)}$$

$$\frac{dP^{b=}_{n,i}}{dt} = k_{H,lin}H_2R^l_{n,0} \quad \text{(A7a)}$$

$$\frac{dP^b_{n,i}}{dt} = k_{H,CGC}H_2R^b_{n,i} \quad \text{(A7b)}$$

Note that in the dead chain generating reactions we distinguish dead chains as originating from Et[Ind]$_2$ZrCl$_2$ (upper index l) or from CGC−Ti (upper index b). The total population of dead chains is simply the sum of both populations: $P^{=}_{n,i} = P^{b=}_{n,i} + P^{l=}_{n,0}$. Usually, we will not make use of this distinction, since both dead chain types are assumed to be equally reactive. Therefore, they are not distinguished in the TDB propagation reactions. However, when describing the characteristics of the dead chain distribution with respect to branching, it is useful to employ the distinction, as will be made clear in the main text. In general, distributions at the two different catalysts are different. However, distributions without and with terminal double bond have *identical shapes*. This can directly be inferred from eqs A6 and A7, showing that the generation terms at rhs are identical. The consumption of the chains with TDB (by the branching reaction) does not affect their distribution shape, only their concentration. Note finally that for completeness we included $P_{n,0}$ in the equations, but due to our assumption that $k_{H,lin} = 0$, in fact this distribution is not created in our calculations.

Population Balances of Growing Chains at Both Catalysts and Polymer Chains without and with a Terminal Double Bond. These are obtained from the full 2-D equations by summing over the number of branches *i*.

$$\frac{dR^l_n}{dt} = k_{i,lin}MC^*_{lin}\delta(n-1) + k_{p,lin}(R^l_{n-1} - R^l_n)M - (k_{\beta,lin} + k_{d1,lin} + k_{m,lin}M + k_{H,lin}H_2)R^l_n \quad \text{(A8)}$$

$$\frac{dR^b_n}{dt} = k_{i,CGC}MC^*_{CGC}\delta(n-1) + k_{p,CGC}(R^b_{n-1} - R^b_n)M - (k_{\beta,CGC} + k_{d1,CGC} + k_{m,CGC}M + k_{H,CGC}H_2)R^b_n + k_{p,TDB}(-\mu^{=}_0 R^b_n + \sum_{m=1}^{n-1} P^{=}_m R^b_{n-m}) \quad \text{(A9)}$$

$$\frac{dP^{l=}_n}{dt} = (k_{m,lin}M + k_{\beta,lin} + k_{d1,lin})R^l_n - k_{p,TDB}P^{l=}_n\lambda^b_0 \quad \text{(A10a)}$$

$$\frac{dP^{b=}_n}{dt} = (k_{m,CGC}M + k_{\beta,CGC} + k_{d1,CGC})R^b_n - k_{p,TDB}P^{b=}_n\lambda^b_0 \quad \text{(A10b)}$$

$$\frac{dP^l_n}{dt} = k_{H,lin}H_2R^l_n \quad \text{(A11a)}$$

$$\frac{dP^b_n}{dt} = k_{H,CGC}H_2R^l_n \quad \text{(A11b)}$$

These population balance equations have been derived before[14] and reflect the generally accepted mechanisms for mixed metallocene catalyst systems with CGC−Ti. In our model, we employ a simplified approach of the monomer balance, since we will not explicitly deal with monomer concentration. The reason for this is that actual monomer concentrations at catalyst sites are not easily inferred from experiments, since they are subject to solubility and mass transfer constraints. Inspection of the equations presented learns that all of them, except for the monomer balance itself, can be solved for the product k_pM, if we assume propagation coefficients to be equal.[7] Notice that in all terms containing M—other than the propagation term—rate coefficients can be replaced by relative rates to propagation, i.e., $k_{i,lin}M = f_{i,lin}k_pM$. Furthermore, we will apply our model to situations of constant monomer concentration. Hence, it is valid for steady-state operation of a CSTR and for the usual operation strategies of semibatch reactors, where monomer pressure is kept constant. This implies that we solve the steady-state version of the monomer balance, eq A3, after adding a term $(\phi_{M,in} - \phi_{M,out})/V$ to the rhs. Here, $\phi_{M,in}$ and $\phi_{M,out}$ are the molar feed and outlet flows—$\phi_{M,out}$ being zero for a semibatch reactor—and V is the reactor volume. In fact, this term represents the volumetric monomer consumption. Throughout all our CSTR and semibatch simulations we impose a value $k_pM = 500$ s^{-1} in combination with a total initial or feed catalyst concentration $C_{lin,0} + C_{CGC,0} = 4 \times 10^{-6}$ kmol/m^3.[7] Since calculations with the kinetic data set of Table 2 show that the total concentration of growing chains $\lambda^b_0 + \lambda^l_0$ practically equals $C_{lin,0} + C_{CGC,0}$, the simplified monomer balance says that volumetric monomer con-

sumption follows as $(\phi_{M,in} - \phi_{M,out})/V = k_p M(\lambda_0^b + \lambda_0^1) = 0.002$ kmol m^3 s, for both reactor systems. Thus, we see that we can solve the model equations without separately specifying k_p and M.

First Branching Moment Distributions for Growing and Dead Chains. These equations have been derived from the full 2-D equations by multiplying with i and summing over this index. This follows a similar procedure as before on ldPE[2] and poly(vinyl acetate).[1] Note that eq A4 does not have an equivalent in the first and second branching moment equations, since multiplying with the number of branches in this cases of branch-less chains means multiplying with zero; hence, it vanishes.

$$\frac{d\Phi_n^{b1}}{dt} = k_{p,CGC}(\Phi_{n-1}^{b1} - \Phi_n^{b1})M - (k_{\beta,CGC} + k_{d1,CGC} + k_{m,CGC}M + k_{H,CGC}H_2)\Phi_n^{b1} + k_{p,TDB}\sum_{m=1}^{n-1}(\Phi_n^{b1}P_{n-m}^{=} + R_m^b\Psi_{n-m}^{=1} + R_m^bP_{n-m}^{=}) \quad \text{(A13)}$$

Equation A13 is obtained using the derivation in the main text and the result given as eq 9.

$$\frac{d\Psi_n^{=1}}{dt} = (k_{m,CGC}M + k_{\beta,CGC} + k_{d1,CGC})\Phi_n^{b1} - k_{p,TDB}\Psi_n^{=1}\lambda_0^b \quad \text{(A14)}$$

$$\frac{d\Psi_n^{1}}{dt} = k_{m,CGC}H_2\Phi_n^{b1} \quad \text{(A15)}$$

Second Branching Moment Distributions for Growing and Dead Chains. These equations have been derived from the full by multiplying with i^2 and summing over this index. Again eq A4 does not have an equivalent second branching moment equation.

$$\frac{d\Phi_n^{b2}}{dt} = k_{i,CGC}MC_{CGC}^*\delta(n-1) + k_{p,CGC}(\Phi_{n-1}^{b2} - \Phi_n^{b2})M - (k_{\beta,CGC} + k_{d1,CGC} + k_{m,CGC}M + k_{H,CGC}H_2)\Phi_n^{b2} + k_{p,TDB}\sum_{m=1}^{n-1}\Phi_m^{b2}P_{n-m}^{=} + R_m^b\Psi_{n-m}^{=2} + 2\Phi_m^{b1}\Psi_{n-m}^{=1} + 2\Phi_m^{b1}P_{n-m}^{=1} + 2R_m^b\Psi_{n-m}^{=1} + R_m^bP_{n-m}^{=} \quad \text{(A16)}$$

Equation A16 is obtained using the derivation in the main text, and the result is given as eq 12.

$$\frac{d\Psi_n^{=2}}{dt} = (k_{m,CGC}M + k_{\beta,CGC} + k_{d1,CGC})\Phi_n^{b2} - k_{p,TDB}\Psi_n^{=2}\lambda_0^b \quad \text{(A17)}$$

$$\frac{d\Psi_n^{=2}}{dt} = k_{H,CGC}H_2\Phi_n^{b2} \quad \text{(A18)}$$

References and Notes

(1) Iedema, P. D.; Grcev, S.; Hoefsloot, H. C. J. *Macromolecules* **2003**, *36*, 458−476.
(2) Iedema, P. D.; Wulkow, M.; Hoefsloot, H. C. J. *Macromolecules* **2000**, *33*, 7173−7184.
(3) Wulkow, M. *Macromol. Theory Simul* **1996**, *5*, 393−416.
(4) Soares, J. B. P.; Hamielec, A. E. *Macromol. Theory Simul.* **1996**, *5*, 547−572.
(5) Iedema, P. D.; Hoefsloot, H. C. J. *Macromol. Theory Simul.* **2001**, *10*, 855−869.
(6) Read, D. J.; McLeish, T. C. B. *Macromolecules* **2001**, *34*, 1928−1945.
(7) Beigzadeh, D.; Soares, J. B. P.; Duever, T. A. *Macromol. Rapid Commun.* **1999**, *20*, 541−545.
(8) Costeux, S.; Wood-Adams, P.; Beigzadeh, D. *Macromolecules* **2002**, *35*, 2514−2528.
(9) Iedema, P. D. Invited lecture, presented at the Workshop Polymer Reaction Engineering IV—Engineering Foundation, Palm Beach, FL, 2000.
(10) Iedema, P. D.; Hoefsloot, H. C. J. *Macromol. Theory Simul.* **2001**, *10*, 870−880.
(11) Iedema, P. D.; Hoefsloot, H. C. J. *Chimia* **2001**, *55*, 256−258.
(12) Lai, S. Y.; Wilson, J. R.; Knight, G. W.; Stevens, J. C.; Chum, P. W. S. U.S. Patent 5,272,236; *Chem. Abstr.* **1993**, 193218e.
(13) Lai, S. Y.; Wilson, J. R.; Knight, G. W.; Stevens, J. C. U.S. Patent 5,665,800, 1997.
(14) Beigzadeh, D.; Soares, J. B. P.; Hamielec, A. E. *Polym. React. Eng. J.* **1997**, *5*, 141−180.
(15) Beigzadeh, D.; Soares, J. B. P.; Hamielec, A. E. *Polym. J. Appl. Polym. Sci.* **1999**, *71*, 1753.
(16) Beigzadeh, D.; Soares, J. B. P.; Duever, T. A.; Hamielec, A. E. *Polym. React. Eng. J.* **1999**, *7*, 195−205.
(17) Beigzadeh, D.; Soares, J. B. P.; Duever, T. A. *Macromol. Symp.* **2001**, *173*, 179−194.
(18) Malmberg, A.; Kokko, E.; Lehmus, P.; Löfgren, B.; Seppälä, J. V. *Macromolecules* **1998**, *31*, 8448−8454.
(19) Kolodka, E.; Wang, W.-J.; Charpentier, P. A.; Zhu, S.; Hamielec, A. E. *Polymer* **2000**, *41*, 3985−3991.
(20) Zhu, S.; Li, D. *Macromol. Theory Simul.* **1997**, *6*, 793−803.
(21) Bick, D. K.; McLeish, T. C. B. *Phys. Rev. Lett.* **1996**, *76*, 14, 2587−2590.
(22) Wang, W.-J.; Yan, D.; Zhu, S.; Hamielec, A. E. *Macromolecules* **1998**, *31*, 8677−8683.
(23) Soares, J. B. P. *Macromol. Theory Simul.* **2002**, *11*, 184−198.
(24) Dekmezian, A. H.; Soares, J. B. P.; Jiang, P.; Garcia-Franco, C. A.; Weng, W.; Fruitwala, H.; Sun, T.; Sarzotti, D. M. *Macromolecules* **2002**, *35*, 9586−9594.
(25) Simon, L. C.; Soares, J. B. P. *Macromol. Theory Simul.* **2002**, *11*, 222−232.
(26) Costeux, S. *Macromolecules* **2003**, *36*, 4168−4187.
(27) Spiegel, M. R. *Theory and Problems of Probability and Statistics*; McGraw-Hill: New York, 1992.

MA034405Q